Carbohydrate Polymers 336 (2024) 122105

Contents lists available at ScienceDirect

Carbohydrate Polymers

journal homepage: www.elsevier.com/locate/carbpol

All-polysaccharide, self-healing, pH-sensitive, *in situ*-forming hydrogel of carboxymethyl chitosan and aldehyde-functionalized hydroxyethyl cellulose

Rafael F.N. Quadrado [a], Zhenghao Zhai [b], Matheus Zavadinack [c], Giseli Klassen [d], Marcello Iacomini [c], Kevin J. Edgar [b,e], André R. Fajardo [a,*]

[a] Laboratório de Tecnologia e Desenvolvimento de Compósitos e Materiais Poliméricos (LaCoPol), Federal University of Pelotas, 96010-900 Pelotas, RS, Brazil
[b] Macromolecules Innovation Institute, Virginia Tech, Blacksburg, VA 24061, USA
[c] Department of Biochemistry and Molecular Biology, Paraná Federal University, 81531-980 Curitiba, PR, Brazil
[d] Department of Basic Pathology, Paraná Federal University, 81531-980 Curitiba, PR, Brazil
[e] Department of Sustainable Biomaterials, Virginia Tech, Blacksburg, VA 24061, USA

ARTICLE INFO

Keywords:
Polysaccharide derivatives
All-polysaccharide hydrogel
Fast gelation
Self-healing
pH responsiveness

ABSTRACT

In situ forming hydrogels are promising for biomedical applications, especially in drug delivery. The precursor solution can be injected at the target site, where it undergoes a sol-gel transition to afford a hydrogel. In this sense, the most significant characteristic of these hydrogels is fast gelation behavior after injection. This study describes an all-polysaccharide, rapidly *in situ*-forming hydrogel composed of carboxymethyl chitosan (CMCHT) and hydroxyethyl cellulose functionalized with aldehyde groups (HEC-Ald). The HEC-Ald was synthesized through acetal functionalization, followed by acid deprotection. This innovative approach avoids cleavage of pyran rings, as is inherent in the periodate oxidation approach, which is the most common method currently employed for adding aldehyde groups to polysaccharides. The resulting hydrogel exhibited fast stress relaxation, self-healing properties, and pH sensitivity, which allowed it to control the release of an encapsulated model drug in response to the medium pH. Based on the collected data, the HEC-Ald/CMCHT hydrogels show promise as pH-sensitive drug carriers.

1. Introduction

Hydrogels are three-dimensional (3D) materials with a high capacity to absorb water and tailored mechanical properties (Sun Han Chang et al., 2019), making them useful for different biomedical applications including drug delivery (de Freitas et al., 2020), tissue engineering (Bertsch et al., 2022), and wound healing (Jiang et al., 2021). The preparation of hydrogels using natural polysaccharides is attractive since they are abundant, benign, and biodegradable (in the cases of unmodified and some modified polysaccharides) (Sánchez-Morán et al., 2019). A convenient administration route of polysaccharide-based hydrogels to patients is by injection of precursors in solution, undergoing conversion to gel at the application site (Meng et al., 2019). This type of *in situ* forming material has many advantages over traditional preformed hydrogels for biomedical applications (Meng et al., 2019). For instance, *in situ* forming hydrogels are readily injectable since the precursor solution is a fluid of low viscosity that can be extruded through a syringe-needle system without clogging issues, becoming a gel-like material only at the target location (Dimatteo et al., 2018). These characteristics permit filling irregular-shaped and deep lesion sites, as well as better mouldability of the hydrogel to those sites, potentially improving biocompatibility with the surrounding tissue (Meng et al., 2019).

Many of the benefits associated with *in situ* forming polysaccharide hydrogels are related to the fast gelation of the precursor solution. Gelation must be sufficiently fast to avoid excessive spreading of the solution (and incorporated drugs) at the injection site, and gelation must not occur during application, thus, avoiding needle-clogging (Dimatteo et al., 2018). To comply with these requirements, dynamic covalent crosslinking has been exploited to prepare *in situ* forming hydrogels. Such reactions are often rapid and result in materials with self-healing ability (Lee et al., 2019). Among dynamic chemistries used for this

* Corresponding author.
E-mail address: andre.fajardo@ufpel.edu.br (A.R. Fajardo).

https://doi.org/10.1016/j.carbpol.2024.122105
Received 18 November 2023; Received in revised form 25 March 2024; Accepted 26 March 2024
Available online 29 March 2024

purpose, Schiff base formation has many attractive features; fast reaction kinetics, no need for catalysts, and the fact that the reaction neither involves toxic crosslinkers nor produces toxic byproducts, yielding only water as a co-product (Hozumi et al., 2018). Schiff base formation occurs between aldehydes or ketones and amine functional groups (amine, hydrazide, or alkoxyamines), affording imine (–C=N–), hydrazone (–C=N-NH–), or oxime (–C=N-O–) bonds, respectively (Chen et al., 2020). Interestingly, the type of amine-containing reactant affects the stability of the formed bond, while Schiff base formation kinetics are controlled by the nature of the carbonyl group (Patenaude et al., 2014). Ketones are less reactive in Schiff base formation than aldehydes due to the additional electron-donating carbon adjacent to the carbonyl group, decreasing electrophilicity while narrowing approach angles (Patenaude et al., 2014).

Thus, for *in situ*-forming hydrogels, polysaccharides containing aldehyde groups are preferred. Typically, the introduction of aldehyde groups to polysaccharides is by periodate oxidation of vicinal diols, creating ring-opened dialdehydes (Chen et al., 2020). This causes reduced rigidity and some degradation during oxidation, which decreases the degree of polymerization (DP) and introduces chemical instability due to the breaking of the pyranose ring (Nichols et al., 2020). Alternatively, appending reactive moieties containing aldehyde groups to the polysaccharide may overcome some of the disadvantages associated with periodate oxidation. However, the direct introduction of reactive, aldehyde-containing moieties is problematic, since they may react, for example, with abundant polysaccharide alcohols (binding the aldehyde into hemiacetal and acetal structures) (Chen et al., 2020). Instead, an interesting approach for this challenge is to append protected aldehyde groups that can be deprotected to free aldehydes. Chemically, this can be done through acid-labile acetal moieties, which can be easily hydrolyzed in a weak acid medium to unmask the aldehydes. This simple chemistry should avoid the destruction of monosaccharide rings, and avoid introducing chemical instability, although some DP loss during the introduction of the protected aldehyde is possible, depending on the conditions used (Baker et al., 2017). Despite its usefulness, this approach has previously been applied only for polysaccharides containing carboxyl groups (Silva et al., 2021; Zeng et al., 2016), where the acetals must have an amine group for further coupling. No efficient method has been developed for non-ionic polysaccharides. Here we present an approach based on this strategy to prepare a non-ionic polysaccharide containing aldehyde groups, capable of forming hydrogels. Our hypothesis is that this approach will reduce the risk of a significant reduction in the DP, prevent damage to the pyranose ring, and avoid introducing chemical instability to the resulting derivative.

We attempted the preparation of an all-polysaccharide, *in situ*-forming hydrogel crosslinked by Schiff imine bonds between aldehydes and amines. Hydroxyethyl cellulose (HEC) was selected as an aldehyde-containing polysaccharide due to its commercial availability, low toxicity, non-immunogenicity, high water solubility, and non-ionic character (Yin et al., 2022). Our approach was to functionalize HEC with acetal-containing moieties, which we anticipated could be hydrolyzed under mild acid conditions to afford an aldehyde-pendant HEC (HEC-Ald). We predicted that acetal functionalization would happen primarily at the termini of the oligo(hydroxyethyl) groups, which have wider approach angles and thus are more reactive than glucose ring hydroxy. Once appended and unmasked, the aldehydes should also be reactive for the same reason, promoting fast gelation. Carboxymethyl chitosan (CMCHT) was chosen as the amine-containing polysaccharide partner because of its solubility even in neutral or slightly alkaline aqueous media (Zhou et al., 2023). CMCHT is biocompatible with many tissues in many circumstances, has low toxicity, and possesses well-known antibacterial, antioxidant, and hemostatic properties (Zhou et al., 2023). We hypothesize that HEC-Ald and CMCHT solutions will readily gel when mixed, allowing the preparation of *in situ* forming hydrogels. We further hypothesize that the prepared hydrogels will be dynamic, pH-sensitive, self-healable, mechanically robust, able to control the release of drugs, and will exhibit low cytotoxicity.

2. Experimental

2.1. Materials

Chitosan (CHT, M_v of 190–310 kDa according to the manufacturer, and a degree of acetylation of 24 % (DS(Ac) 0.24) as measured ^{1}H NMR; Fig. S1) was purchased from Sigma-Aldrich. Hydroxyethyl cellulose (HEC, M_w of 105 kDa determined through SEC analysis, molar substitution (MS) 2.5 according to manufacturer) was purchased from Spectrum Chemical (USA). HEC degree of substitution (DS) was determined by ^{1}H NMR analysis of perpropionylated HEC (Fig. S2); DS(HEC) 1.52. Sodium hydroxide, sodium bicarbonate, sodium chloride, sodium acetate, sodium iodide, sodium hydride, sodium cyanoborohydride, potassium chloride, potassium dihydrogen phosphate, potassium hydrogen phosphate, propionic anhydride, Cibacron Blue 3G-A, monochloroacetic acid, isopropyl alcohol (IPA), hydrochloric acid, dimethylformamide were purchased from Sigma-Aldrich and used as received. 2-Chloroacetaldehyde dimethylacetal, *tert*-butylamine, and vanillin were purchased from Across Organics and used as received. All solvents were dried with molecular sieves overnight prior to use. Dialysis tubing Spectra/Por 7 (MWCO 3.5 kDa) was acquired from Thermo Fischer Scientific.

2.2. General procedure for synthesis and acid deprotection of acetal-functionalized hydroxyethyl cellulose (HEC-ACETAL)

HEC (0.50 g; 1.63 mmol anhydroglucose units (AGU), 4.98 mmol –OH) was dissolved in DMF (20 mL) for 2 h at 60 °C. After cooling to room temperature (RT), NaOH (1.95 g, 10 equiv./–OH; ground to a powder and previously dispersed in a small amount of DMF (~5 mL)) was added to the system under N_2. Then, 2-chloroacetaldehyde dimethyl acetal (8 mL, 15 equiv./–OH) was added dropwise to the solution. Finally, NaI (9 g, 1 equiv./Acetal) was added to the reaction medium, and the formed heterogeneous solution was vigorously stirred for 48 h at 70 °C under N_2. Subsequently, the reaction mixture was dialyzed against deionized water for 48 h (water was exchanged twice a day). The purified acetal-functionalized HEC (HEC-Acetal) was recovered by freeze-drying as a brownish foam-like material. Yield: 70 % (0.35 g, 1.40 mmol AGU). ^{1}H NMR (500 MHz, D_2O): 4.50 (H 1, anomeric proton), 4.01–3.03 (cellulose backbone protons, –OC$\underline{H_2}$C$\underline{H_2}$– protons of oligo(hydroxyethyl) groups, –OC$\underline{H_2}$C$\underline{H}$(OC$\underline{H_3}$)$_2$ and –OCH$_2$CH(OC$\underline{H_3}$)$_2$ protons from the acetal moieties), 3.55 (–OCH$_2$CH(OC$\underline{H_3}$)$_2$ methyl protons from the acetal moieties).

The acetal moieties of HEC-Acetal were converted to aldehyde groups by acid hydrolysis. Briefly, HEC-Acetal (0.50 g) was solubilized in diluted HCl (20 mL, 0.2 mol/L, pH ~ 1.30) under stirring for 8 h at 80 °C. Then the solution was cooled to RT, then neutralized by adding drops of $NaHCO_3$ solution (5 % w/w) with vigorous stirring. The neutralized solution was dialyzed against deionized water for 48 h (water was exchanged twice a day). The product (HEC-Ald) was recovered by freeze drying at −55 °C under reduced pressure (0.014 mbar) for 96 h. Yield: 64 % (0.32 g, 1.70 mmol AGU). ^{1}H NMR (500 MHz, D_2O): 9.50 (C$\underline{H}$O proton), 4.90 (C$\underline{H}$(OH)$_2$ proton), 4.50 (H 1, anomeric proton), 4.01–3.03 (cellulose backbone protons, –OC$\underline{H_2}$C$\underline{H_2}$– protons of oligo(hydroxyethyl) groups and –OC$\underline{H_2}$CH(OH)$_2$ protons from the functionalized aldehyde moieties).

2.3. Identification and quantification of aldehyde groups in HEC-Ald

Identification and quantification of the aldehyde groups in HEC-Ald followed a procedure described by Nichols et al. (2020) with minor modifications. Briefly, HEC-Ald (0.02 g, 0.12 mmol AGU) was solubilized in DMF (1.30 mL) for 2 h at 60 °C. Then, the primary amine *tert*-butylamine (0.38 mL, 30 equiv. per AGU) was added to the solution,

which was then stirred for 24 h at 50 °C. Thereafter, $NaBH_3CN$ (0.075 g, 10 equiv. per AGU) was added to the solution. The resultant mixture was stirred for 24 h at RT. Then, the mixture was added to cold acetone (20 mL), filtered, and the obtained precipitate was extensively washed with ethanol to recover the product, which was dried under vacuum overnight at 50 °C. Yield: 80 % (0.016 g, 0.062 mmol AGU). ^{1}H NMR (500 MHz, D_2O): 4.50 (H 1, anomeric proton), 4.01–3.03 (cellulose backbone protons, –OC$\underline{H_2}$C$\underline{H_2}$– protons of oligo(hydroxyethyl) groups and –OC$\underline{H_2}$C$\underline{H_2}$N$(CH_3)_3$ protons), 2.92–2.00 (DMF and acetone residues), 1.24 (N$(C\underline{H_3})_3$ protons). The NMR spectrum of the recovered product, along with the method used to estimate the DS of tert-butylamine, can be found in the Supporting Information. In this instance, the value of the DS for tert-butylamine is equivalent to the DS for aldehyde.

2.4. Synthesis of CMCHT

CMCHT was synthesized according to a modified procedure reported by Zhou et al. (2023). NaOH (5.40 g) was dissolved in a mixture of IPA (32 mL) and deionized water (8 mL). After complete dissolution, chitosan (4.00 g) was added, and the heterogeneous mixture was stirred for 1 h at 50 °C. Then, chloroacetic acid (6.00 g) in IPA (8 mL) was added dropwise. After stirring for 4 h at 50 °C, an ethanol/water mixture (70 % v/v, 80 mL) was added to precipitate the product, which was recovered by vacuum filtration, and extensively washed with ethanol/water (80 % v/v, 200 mL, four washings). The washed solid product was dissolved in deionized water (100 mL), and centrifuged (8000 rpm, 6 min) to remove insoluble materials. Finally, the centrifuged solution was dialyzed against deionized water (2 L) for 48 h, and the purified CMCHT was recovered by freeze-drying. Yield: 60 % (2.43 g). ^{1}H NMR (500 MHz, D_2O): 4.46 (H 1, anomeric proton), 3.90 (–OC$\underline{H_2}$COOH), 3.80–3.30 (chitosan backbone (GlcN and GlcNAc) protons), 3.29 (–NC$\underline{H_2}$COOH), 2.65 (H 2, GlcN), 1.99 (–NCOC$\underline{H_3}$ protons).

2.5. General procedure for preparation of HEC-Ald/CMCHT hydrogels

Certain amounts of HEC-Ald and CMCHT were dissolved separately in phosphate buffer (pH 7.4) using vigorous stirring. Thereafter, equal amounts of these solutions (0.20 mL) were mixed, briefly vortexed, and immediately incubated in a water bath at 37 °C. Successful gelation and gelation time (t_{gel}) were determined by vial inverting, where the lack of solution flow within 30 s was used as the criterion to define the gel state. Total solid content (5, 10, 15 %) and polysaccharide weight ratio (5:1, 1:1, 1:5) were varied to identify the best gelation conditions. Different concentrations of the HEC-Ald and CMCHT solutions were used, mixing equal amounts to afford hydrogels, as specified above. Table S3 summarizes formulations and compositions tested.

2.6. Characterization

All analyses and procedures can be found in the Supplementary Material.

2.7. Drug encapsulation and release experiments

Vanillin was selected as a model drug to investigate hydrogel encapsulation and release properties. Vanillin-loaded hydrogels were prepared using the experimental procedure detailed in Section 2.5 with some modifications. Briefly, equal amounts of CMCHT (0.5 mL, 12.5 % w/v) and HEC-Ald (0.5 mL, 2.5 % w/v) solutions in PBS (pH 7.4) were mixed to form hydrogel samples; but prior to mixing, vanillin (10 mg, 5 % of total polysaccharide weight) was added directly to HEC-Ald solution, which was sonicated for 10 min. After mixing, gelation occurred within 1 min. Loaded hydrogels were frozen and freeze-dried. Vanillin encapsulation was *ca.* 0.025 mg/mg hydrogel.

For the release experiments, dry hydrogel samples (100 mg) were placed into dialysis tubing (MWCO 3.5 kDa), previously immersed in release medium for 1 h. The ends of the dialysis tubing were tightly closed using nylon strings. Then, the hydrogel sample in dialysis tubing was completely immersed in release medium (20 mL), which was stirred constantly at 37 °C. These experiments employed pH 1.2 (NaCl-HCl buffer), pH 5.2 (acetate buffer), or pH 7.4 (phosphate buffer solution, PBS). At pre-determined time intervals, aliquots (3 mL) were withdrawn and replaced by the respective fresh buffer solution. Aliquots were analyzed in an Evolution 300 UV–Vis spectrophotometer; vanillin concentration was determined using a calibration curve in the appropriate buffer solution. All these experiments were performed in triplicate.

2.8. Cell culture and treatment for viability assay

Normal immortalized breast cells (HB4a) (Stamps et al., 1994) were cultivated in RPMI1640 medium (Gibco) supplemented with 10 % fetal bovine serum (Gibco) at 5 % CO_2 and 37 °C in a humidified atmosphere. Approximately 5×10^3 cells/well were plated in a 96 well plate and treated with 0 (control), 0.1, or 0.01 mg/mL extracts of HEC-Ald/CMCHT hydrogel for 24 h. The extracts were prepared by grinding the hydrogel, followed by dissolution in deionized water to prepare solution with concentrations of 0.1, and 0.01 mg/mL. Cell viability was measured by MTT assay through optical density analysis (van de Loosdrecht et al., 1994). Reduced optical density means lower cell density *vs.* control. Results are averages from experiments performed in triplicate.

3. Results and discussion

3.1. Optimization of HEC-Acetal synthesis and acid-catalyzed deprotection

Our approach was to functionalize HEC with an acetal moiety, the precursor to reactive aldehyde groups through acid hydrolysis while maintaining the HEC polysaccharide structure (Scheme 1). HEC hydroxy groups were reacted with 2-chloroacetaldehyde dimethyl acetal through a simple etherification reaction after deprotonation using NaOH. This strategy allows the functionalization of non-ionic polysaccharides with acetal groups, which seems not to have been heavily explored previously.

First, the synthesis of HEC containing acetal moieties (labeled as HEC-Acetal) was optimized to maximize DS (Table 1). We initially reacted HEC with 2-chloroacetaldehyde dimethyl acetal using NaOH as a base (Table 1, entry 1). No reaction occurred under these conditions, as indicated by the absence of any new signal in the product ^{1}H NMR spectrum (Fig. S3). This could result from competing elimination reactions taking place in the reaction medium, expected for displacement reactions under strong alkaline conditions (Lachia et al., 2011). An effective way to favor displacement over elimination is using a better leaving group. In this way, we added NaI to the reaction medium to generate *in situ* the more reactive 2-iodoacetaldehyde dimethyl acetal, guided by the Curtin-Hammett principle (Finkelstein, 1910; Gao et al., 2018). Successful displacement (Table 1, entry 2) was supported by the product ^{1}H NMR spectrum (Fig. 1). The main signals and their attributions can be found in Table S1. HEC-Acetal had a new resonance at 3.55 ppm, assigned to acetal methyl protons. Integration of this signal

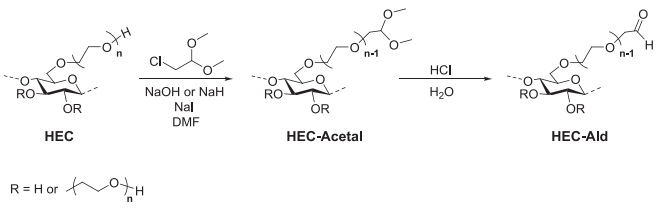

Scheme 1. Illustrative synthesis scheme for HEC-Acetal and HEC-Ald. Structures in this and all schemes are not meant to indicate regioselectivity; they are depicted this way for simplicity and clarity.

Table 1
Conditions tested and results for synthesis of HEC-Acetal.

Entry	Acetal reactant (equiv/–OH)	Base (equiv/ –OH)	NaI (equiv/ Acetal)	DS (Acetal)
1	15	10	–	–
2	15	10	1	0.12
3	15	10	2	0.12
4[a]	15	10	1	0.09
5	20	10	1	0.06
6	10	10	1	–
7	15	5	1	–
8[b]	15	10	1	0.12

[a] NaH used as the base.
[b] Reacted for 96 h. In all other conditions tested, the normal reaction time was 48 h.

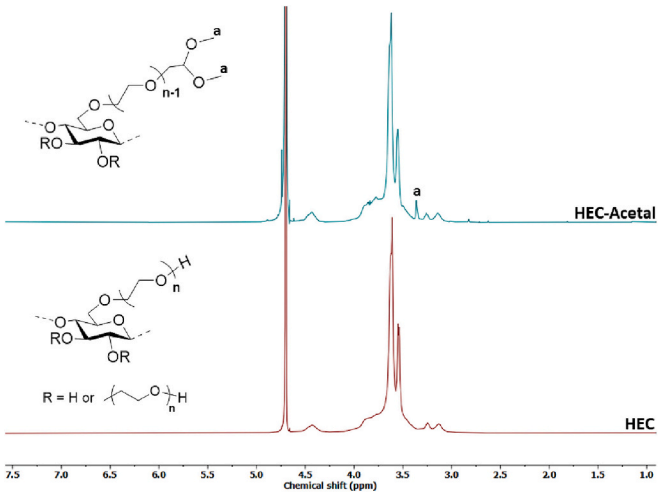

Fig. 1. ^{1}H NMR spectra of HEC and HEC-Acetal (Solvent: D_2O).

allowed the calculation of a modest DS(Acetal) of 0.12. The functionalization was corroborated by ^{13}C, HSQC, and COSY NMR experiments (Figs. S11, S12, and S13, respectively). Increasing NaI equiv. did not increase DS (Table 1, entry 3).

We replaced NaOH with NaH, a stronger base with a higher potential to generate HEC alkoxide groups, seeking to increase DS(Acetal). However, NaH base in the presence of NaI afforded lower DS (Table 1, entry 4). This unexpected result may indicate predominant competing elimination due to high NaH basicity (Barham et al., 2018; Lachia et al., 2011). Thereby defining NaOH as the optimal base, we explored increasing equiv. 2-chloroacetaldehyde dimethyl acetal/OH, but this did not increase DS (Table 1, entry 5). Competitive elimination of the elements of HCl from 2-chloroacetaldehyde dimethyl acetal appeared to be occurring, due to the presence of an acidic acetal C—H (Bentley et al., 1998; Zhao et al., 2009). Indeed, when reduced amounts of 2-chloroacetaldehyde dimethyl acetal were used (10 equiv./–OH), no condensation was observed (Table 1, entry 6; Fig. S8). Lastly, we investigated whether decreasing the amount of NaOH would suppress elimination, favor displacement, and thus enhance DS. However, with less NaOH (5 equiv./–OH), no displacement was seen (Table 1, entry 7; Fig. S9).

Optimal conditions identified for HEC-Acetal synthesis (Table 1) were 15 equiv./–OH of 2-chloroacetaldehyde dimethyl acetal, 10 equiv. NaOH/–OH, and 1 equiv. of NaI/Acetal, with reaction time 48 h (entry 2, Table 1; extending the reaction time to 96 h did not result in higher DS (entry 8)). These optimal conditions afforded DS(Acetal) 0.12. Despite this limitation, this synthetic protocol was able to append acetal moieties to a non-ionic polysaccharide in a feasible manner. We predict that displacement would be favored by using an acetal-containing reagent with a longer polymethylene spacer (*e.g.*, 2–4 carbons) between halide and acetal, since this would remove the possibility of β-elimination and should not impair nucleophilic substitution. Our main goal was hydrogel preparation; we hoped that the DS(Acetal) achieved would be adequate for rapid hydrogel formation if the acetals could be efficiently converted to aldehydes.

Likely, the reaction with 2-chloroacetaldehyde dimethyl acetal occurred primarily at the termini of oligo(hydroxyethyl) groups. The theory supports this supposition: the HEC used has a moderate residual ring –OH (DS 3 − 1.52 = 1.48; and many of these are less reactive 3-OH groups) (Fabbri et al., 2002; Fox et al., 2011). The terminal oligo (hydroxyethyl) hydroxy groups also have wider approach angles and so are much more reactive than ring hydroxy (Abbas, Amin, Hussain, Sher, et al., 2017; Abbas, Amin, Hussain, Sher, et al., 2017; Arukalam et al., 2014).

Next, we explored conditions for acid-catalyzed deprotection of HEC-acetal, using our highest DS(Acetal) polymer (Table 1, entry 2). We employed dilute HCl (0.2 mol/L) to minimize DP loss, expecting that acetal hydrolysis would be facile. Initially, HEC-Acetal was hydrolyzed in solution at 25 °C for 48 h, which resulted in a conversion of the acetal groups to aldehydes of 53 %. ^{1}H NMR spectra of the deprotected HEC-Ald derivatives are shown in Fig. 2. The main signals and their attributions can be found in Table S2. The ^{1}H NMR spectra of these derivatives showed a new resonance at 4.90 ppm due to the α-proton of the hydrated aldehyde (Baker et al., 2017), and reduced intensity of the acetal methyl resonance (highlighted box in Fig. 2), supporting partial deprotection. It is quite common for polysaccharide derivative reactions to show slower kinetics due to issues like narrow approach angles and slow macromolecular diffusion (Deslongchamps et al., 2000).

We next conducted HEC-Acetal deprotection at higher temperatures, while attempting to mitigate any additional DP reduction by reducing reaction time. Deprotection at 50 °C (24 h, dilute HCl) afforded only 50 % conversion, while at 80 °C for 8 h resulted in complete hydrolysis of acetal groups, as is clear from the product ^{1}H NMR spectrum, where the methyl resonance has disappeared. The HEC-Ald displayed only a weak aldehyde proton resonance at 9.50 ppm (*inset* in Fig. 2), undoubtedly due to the hydration of the aldehyde (Baker et al., 2017).

Further evidence that conversion at 80 °C was complete was obtained by reacting HEC-Ald with *tert*-butylamine (Fig. S14). The strong *tert*-butyl methyl proton resonance indicated full conversion (DS(Imine) 0.12 by ratio of *tert*-butyl to backbone integrals). Integration of the aldehyde signals (hydrated and "free" forms) *vs.* the backbone supported this DS. Finally, the full conversion of this HEC-Ald derivative was also corroborated by ^{13}C, HSQC, and HMBC NMR experiments (Figs. S15, S16, and S17, respectively). As expected, M_w of HEC-Ald was reduced *vs.* starting HEC (from 105 to 30.5 kDa). Despite this, the reduction in M_w observed in this case is still lower than the reduction typically observed in some periodate oxidations that introduce a high number of aldehydes. Since the HEC-Ald prepared by deprotection at 80 °C for 8 h had the highest DS(Aldehyde), this derivative was used to prepare hydrogels.

3.2. Synthesis of CMCHT

We prepared CMCHT using conditions (strong base) conducive to *O*- (*vs. N*-) carboxymethylation, to obtain the maximum DS of free amines available for reaction with HEC-Ald. Thus, CMCHT was synthesized by the reaction of CHT with chloroacetic acid in the presence of NaOH since alkoxides compete more effectively as nucleophiles with amines than alcohols. CMCHT structure (in its salt form) was confirmed by ^{1}H NMR (Fig. 3); methylene protons from the carboxymethyl groups in the 3- and 6-*O* positions resonated at 3.90 ppm. Some carboxymethylation also occurred at the 2-amine groups, as evidenced by the resonance at 3.31 ppm (Zhou et al., 2023). By deconvolution of these signals (Fig. S12), combined DS at 3-*O* and 6-*O* was estimated as 1.14, while the DS at the 2-*N* position was determined as 0.38. The DS of free amine groups was calculated as 0.38 by difference (DS(Amine) = 1 – DS(2-*N*-carboxymethyl) – DS(Acetyl)).

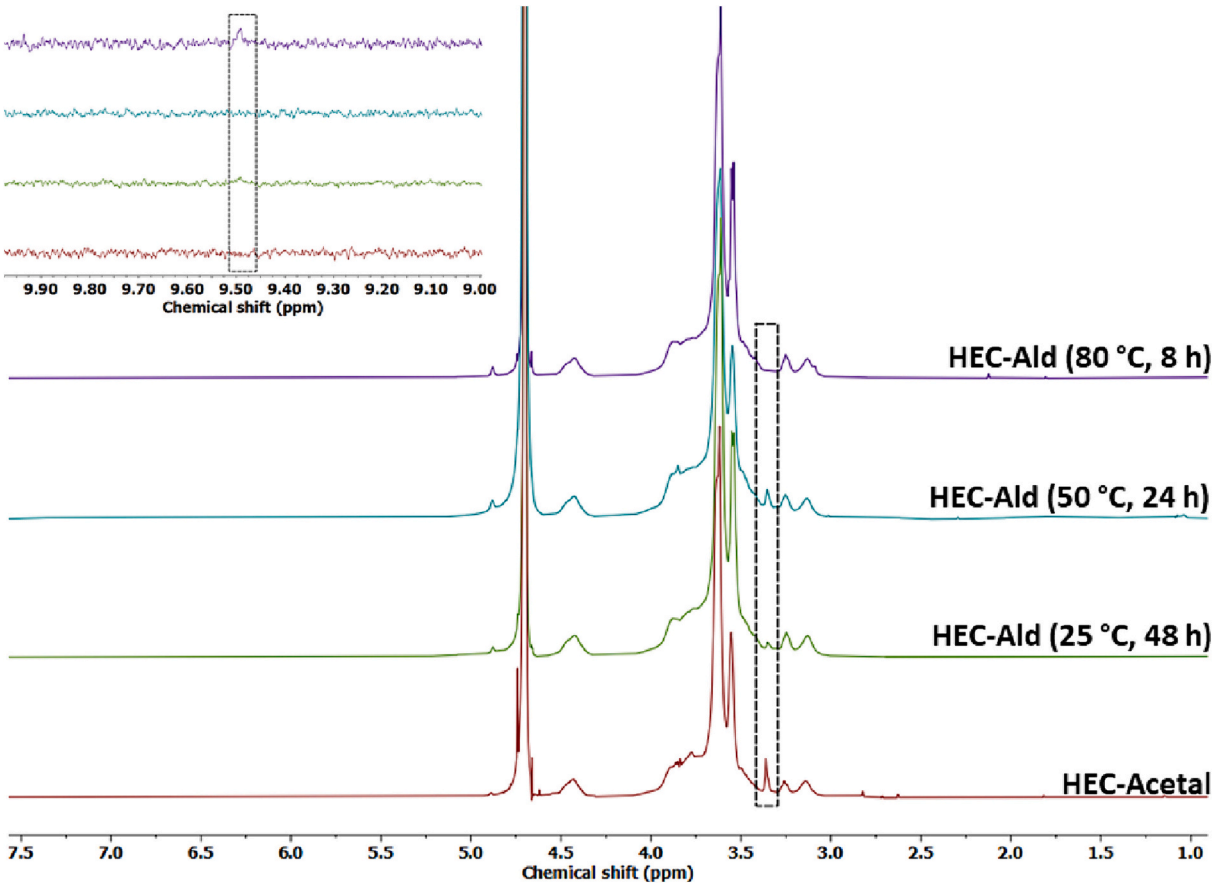

Fig. 2. ^{1}H NMR spectra of HEC-Ald derivatives *vs.* HEC-Acetal. I*nset* shows aldehyde region, magnitude enhanced × 1000 (Solvent: D_2O).

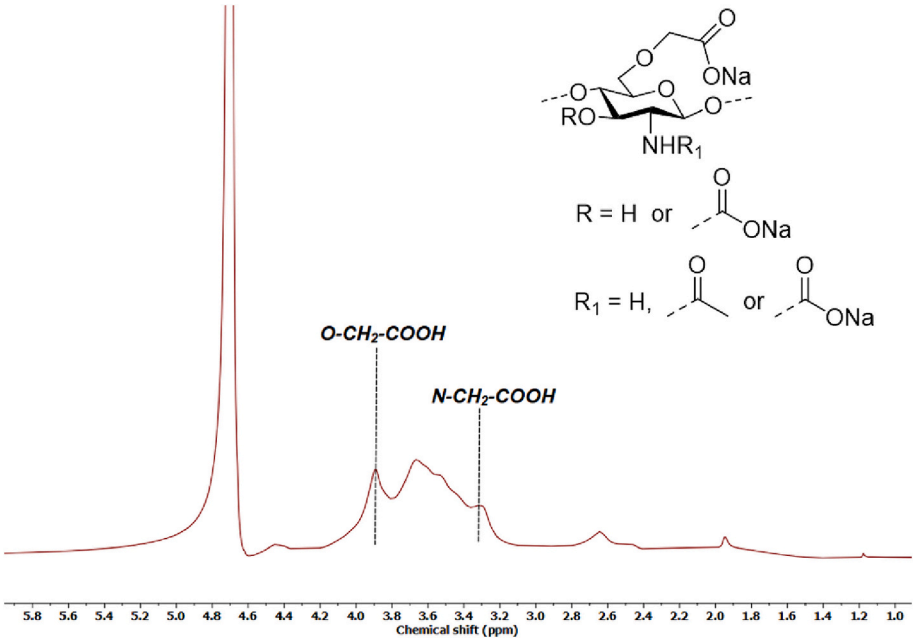

Fig. 3. ^{1}H NMR spectrum of CMCHT (Solvent: D_2O).

3.3. *In situ-forming HEC-Ald/CMCHT hydrogels*

We hoped for rapid reaction kinetics upon mixing CMCHT (amine) and HEC-Ald (aldehyde) solutions, leading to spontaneous gelation and hydrogel formation (Fig. 4a (Zhou et al., 2023)), but had some concerns about the observed hydration of HEC-Ald aldehyde groups (Lázaro Martínez et al., 2010). Guided by Le Chatelier's principle, we hypothesized that consumption of the "free" aldehyde during imine bond formation would shift the equilibrium from acetals and hemiacetals (Bentley et al., 1998; Godoy-Alcántar et al., 2005); the alkaline medium

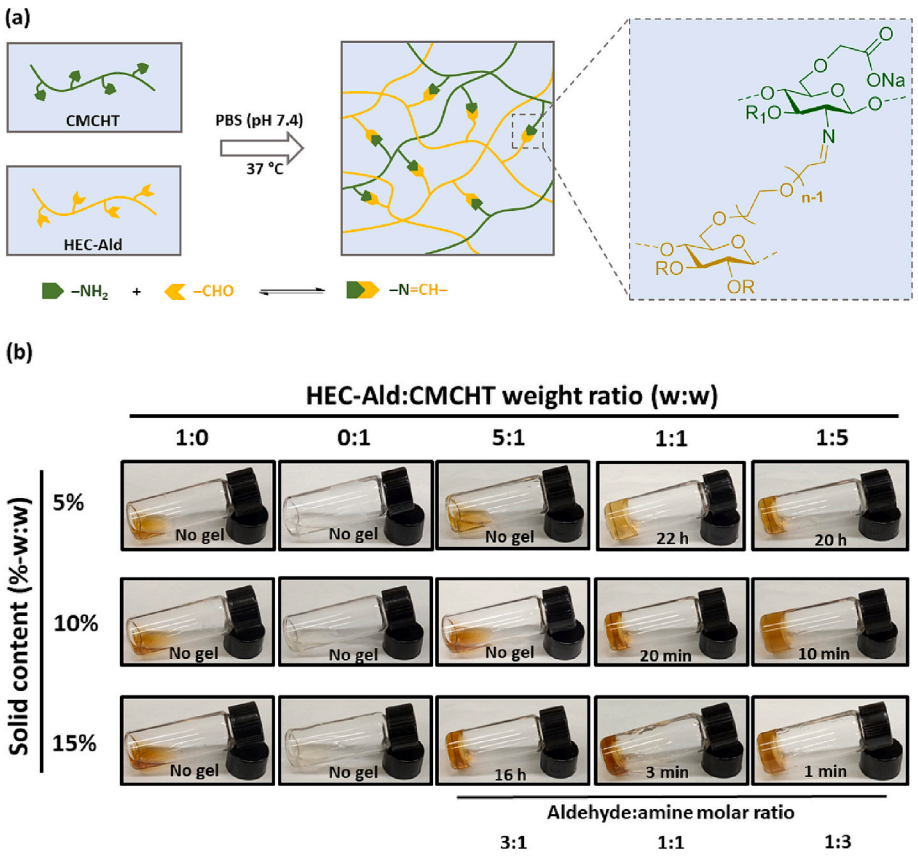

Fig. 4. Illustrative scheme of HEC-Ald/CMCHT hydrogel preparation (a), and summary of experimental conditions tested for its preparation (b). Aldehyde:amine molar ratio is from DS(Aldehyde) and DS(Amine).

also favors free aldehyde (Barnes & Zuman, 1973; Zott et al., 2022). Thus, we hypothesized that performing condensation with amines in slightly alkaline (pH 7.4) PBS would favor imine formation and gelation.

To investigate these hypotheses and meet the fast gelation requirement, the influences of hydrogel formulation solids content and CMCHT: HEC-Ald weight ratio upon gelation time were investigated using PBS (pH 7.4) solvent (Fig. 4b). Control experiments showed that, as expected, both CMCHT and HEC-Ald were necessary for gelation. Secondly, gelation was faster as the proportion of CMCHT in the hydrogel formulation increased, while using an excess of HEC-Ald did not accelerate gelation. This indicated to us that acetal-aldehyde equilibria were not important impediments, consistent with observations about imine formation in small molecule chemistry, where an excess of amine is often required to boost reaction rates (Scheller et al., 2015)[r]. Gelation became faster as hydrogel total solid content increased from 5 % to 15 % (w:w), due to additional hydrogen bonding and entanglements in the highly concentrated solutions that favor imine bond formation and the gelation process (Jiang et al., 2021). Hydrogel crosslink density was studied by analyzing their elastic chain concentration (ν_e), calculated using the Rubber Elasticity Theory (Fig. S19, and Table S4). In general,

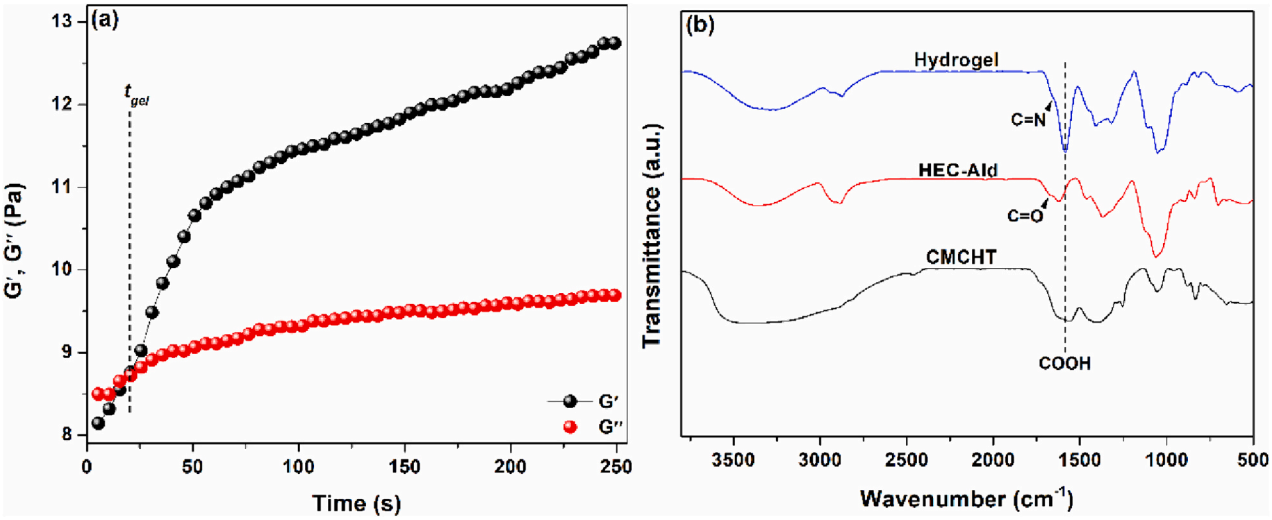

Fig. 5. Time-dependent rheological curves of the HEC-Ald/CMCHT hydrogel (a), and FTIR spectra of CMCHT, HEC-Ald, and of the prepared hydrogel (b).

the elastic chain concentrations of the hydrogels increased with increasing solids content and amount of CMCHT. The solution with a solids content of 15 % (w:w), and HEC-Ald:CMCHT weight ratio 1:5 was able to form a hydrogel within 1 min, an attractive time range for rapid gelation inside the body. Time-dependent rheological experiments were performed with this formulation to gain further insight into gelation kinetics (Fig. 5a**)**.

Fast gelation (Fig. 5a**)** is indicated by the rapid crossover between the storage (G') and loss (G'') moduli, occurring at $t_{gel} = 16$ s. After this stage, G' increases until reaching a plateau due to the development of the crosslinked hydrogel network. The duration of the gelation process (Δt_{gel}) was further evaluated by calculating the time derivative of G' (dG'/dt) during gelation (Fig. S20). Specifically, Δt_{gel} was calculated as the time covering the full width at 40 % of the maximum peak of the Gaussian fitted curve of the derivative of G' (Sun Han Chang et al., 2019). Through analysis of Δt_{gel}, the gelation process starts around 16 s and finishes after 1 min, explaining the different t_{gel} measured by rheology and vial inverting, since in vial inversion t_{gel} is defined when gelation is sufficient to prevent flow upon vial inversion (Ganguly et al., 2018).

The rapid gelation observed in the solutions of CMCHT and HEC-Ald after mixing can also be attributed to the wide approach angles and reactivity of the oligo(hydroxyethyl) terminal aldehyde groups of HEC-Ald. Additionally, the high solid content promotes the formation of auxiliary hydrogen bonds and entanglements, which further facilitate rapid gelation. FTIR was used to confirm the formation of imine bonds between CMCHT and HEC-Ald. The FTIR spectra of the hydrogel and starting polymers (Fig. 5b) show that the hydrogel displays expected bands from CMCHT and HEC-Ald, and a new band at 1657 cm^{-1} assigned to stretching of the C═N bond, confirming imine crosslinking (Lee et al., 2019).

The rapid-gelling (16 s) hydrogel prepared with a solid content of 15 % (w:w) and an HEC-Ald:CMCHT weight ratio of 1:5 provides promise that the solution containing that composition can be injected without risk of needle-clogging, while quickly forming a gel at the application site, limiting spreading of the solution or leaching of encapsulated bioactive molecules. We selected this hydrogel for further characterization.

3.4. Mechanical properties

Biomedical applications of hydrogels depend strongly on their mechanical properties (Chen et al., 2020), which influence the hydrogel's ability to mimic the extracellular matrix and disperse and withstand stress or strain, crucial mechanical support for cell growth and differentiation (Chen et al., 2020). Some studies also indicated a tight link between hydrogel mechanical properties and *in vivo* biocompatibility (Chaudhuri et al., 2016; Dimatteo et al., 2018). Notwithstanding, the reversible nature of the imine crosslinks also should impact HEC-Ald/CMCHT hydrogel mechanical properties, which were investigated by rheology at 37 °C using fresh hydrogel samples, prepared on the rheometer plate. First, the hydrogel was submitted to a strain-sweep experiment at a low frequency (0.5 Hz) to determine its linear viscoelastic regime under shear (Fig. 6a**)**. For most of the strain range tested, G' moduli was much higher than G''. However, G'' progressively increased after a small strain of 10 %, indicating an increment in the viscous character, probably because of the breaking of imine crosslinks as mechanical stress increased (Chen et al., 2020). Eventually, G'' surpassed G' at 250 % strain due to the substantial collapse of the hydrogel network. The HEC-Ald/CMCHT hydrogel was also investigated by a frequency-sweep experiment, employing a small strain value within its viscoelastic regime (1 %; Fig. 6b**)**. G' was higher than G'' throughout the entire range of frequencies investigated. At high frequencies (> 0.4 Hz), however, G'' increased, while G' remained constant. Such behavior indicates an increment in hydrogel viscous character due to breaking of imine bonds under mechanical stress, leading to energy dissipation, and higher G'' (Sánchez-Morán et al., 2019). In short, these results clearly showed the viscoelastic nature of the prepared hydrogel.

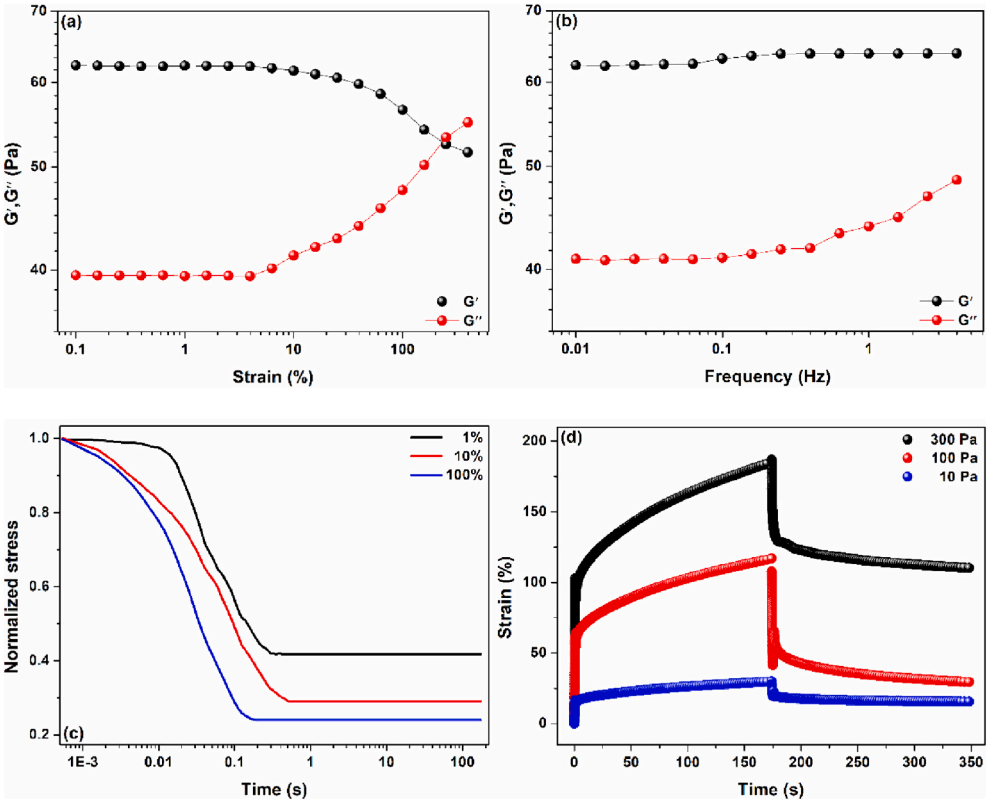

Fig. 6. Strain-sweep (a), frequency-sweep (b), stress relaxation (c), and creep-recovery (d) rheological curves of the prepared HEC-Ald/CMCHT hydrogel.

Owing to the viscoelasticity of HEC-Ald/CMCHT hydrogel and the dynamic nature of its imine crosslinks, we expected that it would show stress relaxation and creep (plasticity/mouldability). Since cells deform and plastically remodel the surrounding extracellular matrix (Bertsch et al., 2022), a hydrogel matrix that does not show such properties can harm the growth of cells and their activity, thereby decreasing the compatibility of the hydrogel with tissues (Bertsch et al., 2022). Stress relaxation of the prepared hydrogel was investigated by rheometry under different strains within the hydrogel linear viscoelastic regime, selected to reflect the broad strain range to which biomaterials may be subjected (Chaudhuri et al., 2016). Stress relaxation results (Fig. 6c) were normalized by the maximum stress after the strain rise step. Stress relaxation was faster as the applied strain increased because, at higher strains, more imine bond crosslinks were broken and rearranged, dissipating energy and stress (Sánchez-Morán et al., 2019). Indeed, this explains the delayed stress relaxation when the HEC-Ald/CMCHT hydrogel was subjected to the lowest strain tested (1 %), as imine rearrangement only happened after the buildup of stress at longer experiment times (Sánchez-Morán et al., 2019). Despite that, stress relaxation occurred in a single step at all strains tested. The general Maxwell model well fit stress relaxation data (Chaudhuri et al., 2016) using only one viscoelastic element (Fig. S21). This behavior is typically associated with a main molecular relaxation event, which must be the rearrangement of imine bonds, and matrix reorganization to disperse stress (Lee et al., 2019). The characteristic stress relaxation times (τ_r) calculated from the Maxwell model fits were 0.083, 0.076, and 0.034 s for the strains of 1 %, 10 %, and 100 %, respectively.

For all strains tested, more than half of the initial stress was relaxed in <1 s. This ultrafast stress relaxation behavior is unprecedented for polysaccharide-based hydrogels. Previous polysaccharide-based hydrogels crosslinked through imine bonds typically showed stress relaxation in the interval of a few seconds (>10 s) to several minutes (Bertsch et al., 2022; Chaudhuri et al., 2016; Liu et al., 2020; Sánchez-Morán et al., 2019). Enhanced reversibility of the imine bond formed by an amine and an aldehyde does not explain entirely the fast stress relaxation observed for the HEC-Ald/CMCHT hydrogel. If most HEC-Ald aldehyde groups are appended to the oligo(hydroxyethyl) termini, they are more reactive, and imine bonds should be broken and reformed at high rates, leading to the ultrafast stress relaxation observed.

Another relevant viscoelastic parameter of biomedical materials is their creep behavior, which can be defined as the tendency of a material to be plastically deformed under stress (Bertsch et al., 2022). The creep potential of a material indicates the ease with which it is remodeled by mechanical stress from cells or any other external source, mimicking natural behaviors in tissues, and increasing integration of the biomaterial with the body (*i.e.*, biocompatibility) (Bertsch et al., 2022). The HEC-Ald/CMCHT hydrogel was submitted to creep-recovery experiments, where an induced strain is measured upon application of constant stress during a time, and after release of the stress in the recovery stage. Due to its effective stress relaxation, the prepared hydrogel should show a low tendency for recovery after stress release due to the rearrangement of imine crosslinks to dissipate the applied stress, also resulting in high induced strain. Experiments reflected a stress range to which biomaterials may be subjected in the human body(Chaudhuri et al., 2016). Under stress, the HEC-Ald/CMCHT hydrogel was instantaneously deformed (Fig. 6d**)** with induced strain increasing as applied stress increased as more imine bonds were broken and reformed. After stress release, the hydrogel did not show a significant strain recovery due to efficient network reorganization, indicating the plasticity and, in a broader sense, mouldability of this hydrogel. The creep behavior of the prepared hydrogel was visually demonstrated by tilting a vial containing the hydrogel and maintaining it horizontally for 1 day (Fig. S22). The hydrogel was flattened due to the force of gravity. When the vial containing the hydrogel was put into a vertical position, the hydrogel maintained its deformation state, demonstrating its creep behavior. Repeating this cycle gave the same results, suggesting the ease with which the hydrogel was plastically deformed and remodeled. All the results obtained from the stress relaxation and creep-recovery experiments indicated that the prepared hydrogel has interesting viscoelastic properties that mimic the natural extracellular matrix, promising compatibility in certain tissues and situations, and potentially boosting cell growth and even cell activity. Finally, the mechanical properties of the HEC-Ald/CMCHT hydrogel were investigated by compression tests (Fig. S23). The hydrogel exhibited a compressive strain until break of 66 ± 2.03 % and Young's modulus of 5.70 ± 0.98 Pa. Table S5 compares mechanical properties of the HEC-Ald/CMCHT hydrogel *vs.* similar polysaccharide-based hydrogels. HEC-Ald/CMCHT hydrogel has a much lower Young's modulus, but a higher compressive yield strain than some other selected hydrogels. Due to its reversible imine crosslinks and network reorganization, the hydrogel is easily deformed by imposed stress (resulting in a lower Young's modulus), withstanding a higher degree of deformation until break. These results further support the viscoelastic nature of the HEC-Ald/CMCHT hydrogel.

3.5. Injectability, adhesive property, and self-healing of the hydrogel

In situ forming hydrogels are advantageous for drug delivery due to their minimally invasive administration, rapidly fitting to irregular target sites or even deep penetrating wounds (Dimatteo et al., 2018). To qualitatively evaluate HEC-Ald/CMCHT hydrogel for drug delivery, an injectability experiment was designed in which equal amounts of CMCHT and HEC-Ald solutions were filled in a double-barrel syringe containing a mixing tip, which had a 20G needle (inner diameter of 0.90 mm) adapted to its end (Fig. 7a**)**. The HEC-Ald solution was mixed with a small amount of blue dye to facilitate visualization. Upon pressure on the plunger, the solutions were extruded through the mixing tip and needle, instantaneously gelling afterward in warm water (~37 °C), although some spilling occurred due to insufficient initial mixing of the solutions (Figs. 7b, c). They were also applied to a collagen membrane in "dry" (Fig. 7d) and "wet" (Fig. 7e) conditions. After rapid gelation, the formed hydrogel was stable and adhered strongly to the membrane, which allowed it to be bent and twisted. These results demonstrated the *in situ* gelation ability of the prepared hydrogel. Furthermore, the shear-thinning capacity of the HEC-Ald/CMCHT hydrogel was evaluated, where was possible to observe that hydrogel viscosity decreased as the shear rate increased (Figs. S24, S25).

Adhesion of hydrogel is also important for various applications, including medical (*e.g.*, application to burns or wounds). This was qualitatively evaluated by placing the hydrogel on a substrate (in this case, a hand covered by a glove), which could be turned upside down, vertically, and bent without resulting in hydrogel detachment (Fig. S26). Quantitative measurements were made through lap-shear experiments in dry and wet conditions (Fig. S27), where the hydrogel was sandwiched between two collagen membranes pressed against each other. By submitting the entire system to vertical extension (*i.e.*, tension testing), the adhesive strength could be estimated. For the wet condition, the collagen membranes were immersed in water before the experiments. In general, the adhesive strength of the hydrogel was much higher in dry (8.30 ± 1.22 kPa) than in wet conditions (4.60 ± 0.64 kPa). The adhesive strength of HEC-Ald/CMCHT (in dry condition) was like that of other polysaccharide-based hydrogels (Table S5).

Due to the dynamic and reversible character of the imine bond crosslinks, the prepared HEC-Ald/CMCHT hydrogel should exhibit self-healing properties, as verified by a visual method. Hydrogel disks (one stained with a blue dye) were prepared, cut, and placed in contact with each other, with no pressure applied. They merged instantaneously into a single piece, which could be easily manipulated by lifting without falling apart (Fig. 8, and Video S1). This self-healing observed is fast in comparison to other imine crosslinked hydrogels that typically require hours to self-heal properly (Chen et al., 2020; Liu et al., 2020; Sánchez-Morán et al., 2019; Zhou et al., 2023), related to the enhanced dynamics of imine bond formation. The self-healing ability of the HEC-Ald/

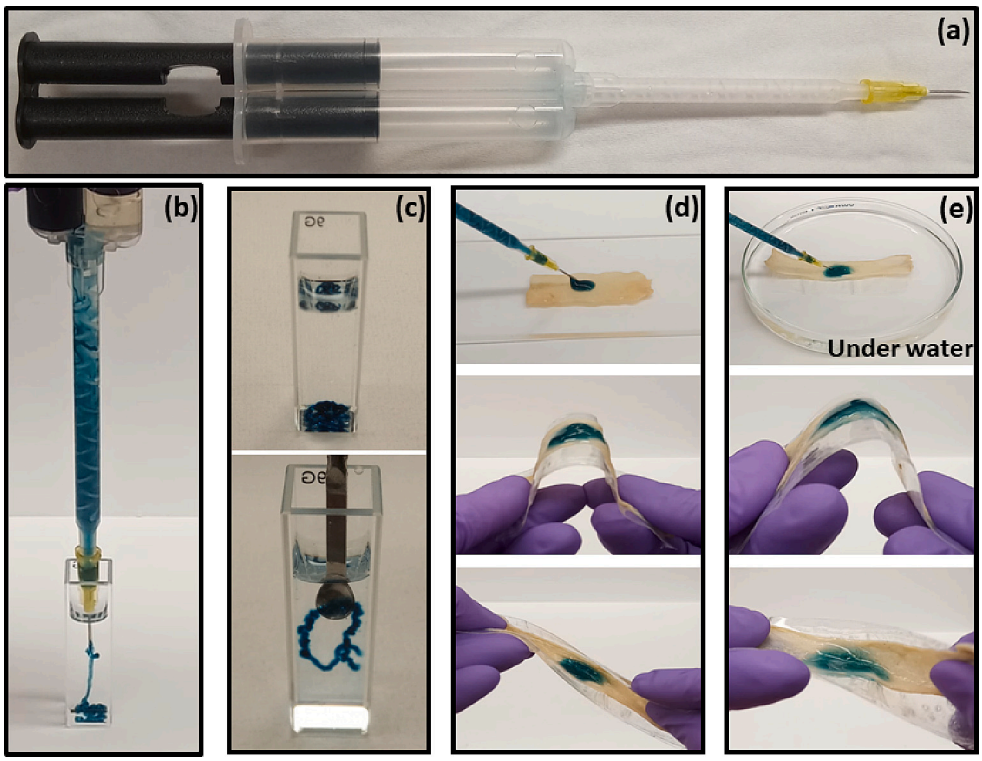

Fig. 7. Photographs of qualitative tests to demonstrate injectability and *in situ* forming ability of the HEC-Ald/CMCHT hydrogel. Injection system used (a) to extrude polysaccharide solutions into warm water at 37 °C (b,c). Hydrogel also was formed when applied directly to a collagen membrane in "dry" (d) or "wet" (e) conditions. HEC-Ald solution was stained with blue dye Cibacron Blue 3G-A to facilitate visualization. (For interpretation of the references to colour in this figure legend, the reader is referred to the web version of this article.)

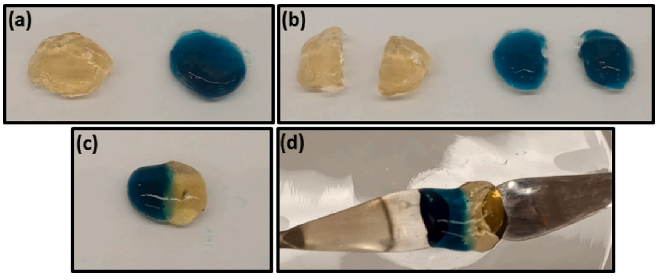

Fig. 8. Self-healing behavior of the prepared HEC-Ald/CMCHT hydrogel, where hydrogel disks were prepared (a), and cut (b). Pieces were placed in contact with each other without pressure (c), and they instantly resisted separation (d). One hydrogel disk was stained with the blue dye Cibacron Blue 3G-A. (For interpretation of the references to colour in this figure legend, the reader is referred to the web version of this article.)

CMCHT hydrogel was also evaluated by step-strain rheometry experiments over a period (Fig. 9). The hydrogel was submitted to sequential strain variation of 1 % to 250 % in segments of 3 min and G' and G'' were measured. At low strain (1 %), G' exceeded G'' indicating the gel state. Increasing strain to 250 % led to G'' surpassing G', indicating disruption of the hydrogel network and fluidization. Upon returning to 1 % applied strain, G' and G'' returned to their original values immediately, suggesting fast reformation of imine crosslinks, restoring the hydrogel network. The full cycle was repeated with the same results twice more, further confirming the self-healing ability of the HEC-Ald/CMCHT hydrogel.

3.6. Swelling and weight loss behaviors

Hydrogel swelling behavior is important for biomedical applications

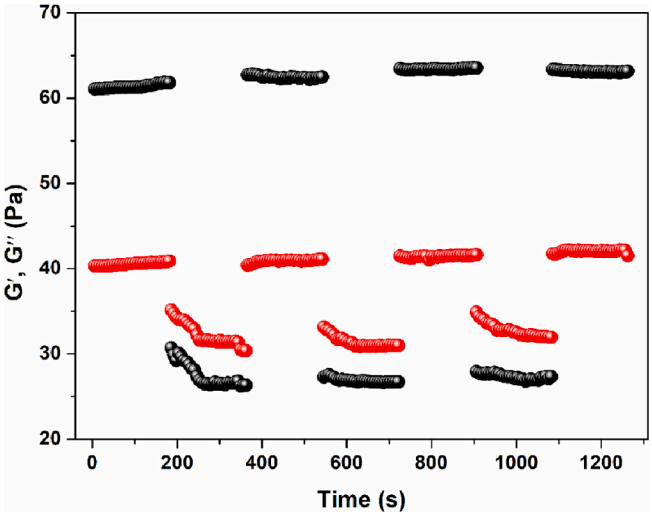

Fig. 9. Step-strain rheological curves of the HEC-Ald/CMCHT hydrogel; strain switched from 1 % to 250 % in intervals of 3 min (180 s) (frequency 1 Hz).

because it influences properties such as stiffness, the ability to entrap cells and induce their proliferation/growth, and the release rate of encapsulated drugs (Yin et al., 2022). Especially for drug release, pH-responsive swelling behavior is important because many wound and cancer sites have distinct pH values that can vary from extremely acidic to alkaline(Yin et al., 2022). The effect of pH on the swelling behavior of the HEC-Ald/CMCHT hydrogel was evaluated at 37 °C using buffer solutions at pH 1.2, 5.2, and 7.4, covering the broad pH range found in many tumors and wound sites (Cao et al., 2019) (Fig. 10a). As pH decreased, the hydrogel swelled faster and to a higher maximum degree;

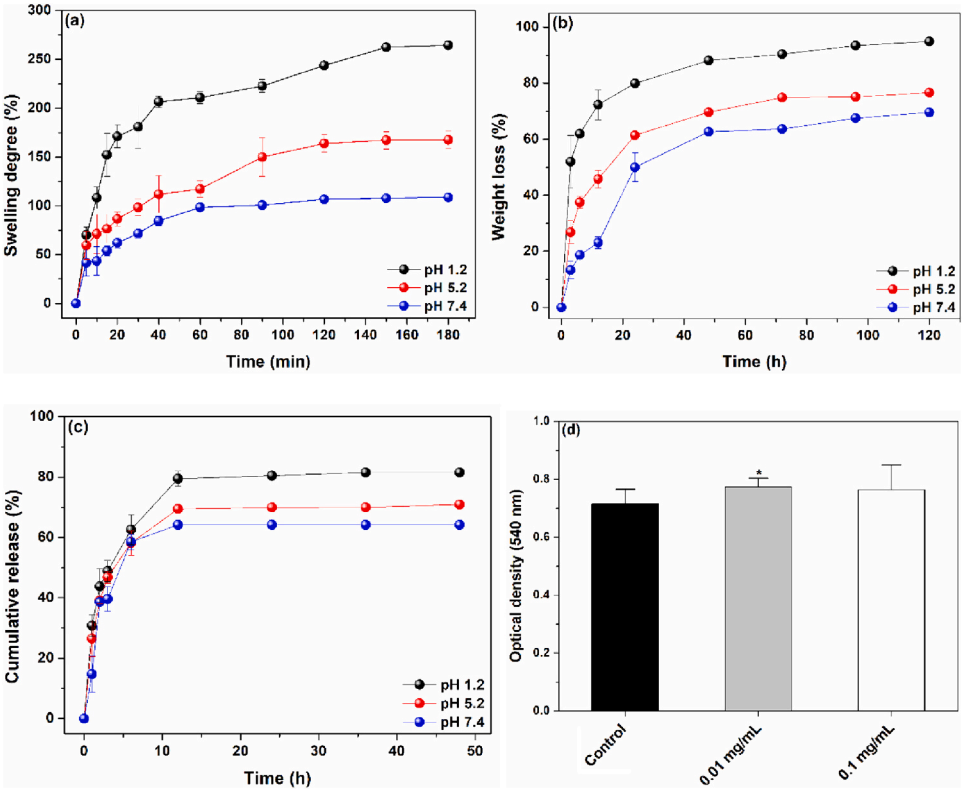

Fig. 10. Swelling (a), weight loss (b), and vanillin release curves (c) of HEC-Ald/CMCHT hydrogel *vs.* pH (37 °C), and cytotoxicity of different hydrogel concentrations against normal HB4a cells (d). *Statistically different from the control experiment ($p < 0.05$).

107 % at pH 7.4, 162 % at pH 5.2, and 265 % at pH 1.2 (all after 180 min). This behavior can be assigned to faster imine hydrolysis under acidic conditions (Chen et al., 2020). As a result, the polymeric network is loosened, allowing the absorption of more liquid, leading to greater swelling. In addition, free CMCHT amines are protonated below about pH 6, so cation-cation repulsion forces contribute to hydrogel expansion and liquid absorption (Yin et al., 2022). Hydrogel stability was evaluated by measuring its weight loss at pH 1.2, 5.2, and 7.4 at 37 °C (Fig. 10b**)**. Hydrogels exhibited higher weight loss as incubation medium pH decreased from pH 7.4 to pH 1.2, due to faster imine hydrolysis at acidic pH, resulting in the leaching of non-crosslinked polymer chains out of the hydrogel matrix. The hydrogel had lost >95 % of its initial weight at pH 1.2 by the end of the experiment, *vs.* only 69 % at pH 7.4. Thus, the hydrogel clearly exhibits pH-sensitive behavior, as evidenced by its swelling and weight loss characteristics. This behavior could prove useful in controlling the release of encapsulated bioactive compounds, triggered by changes in tissue pH.

3.7. *In vitro* drug release

The potential of the HEC-Ald/CMCHT hydrogel in DDS was investigated through encapsulation and subsequent release of vanillin, selected as a model drug due to its high UV–Vis absorption, allowing easy quantification. Vanillin has been reported to possess interesting bioactivity, including anticancer, antiviral, antimicrobial, and antioxidant properties (Arya et al., 2021). A vanillin-loaded hydrogel was prepared by simply adding the drug to the HEC-Ald solution before mixing it with the CMCHT solution. Vanillin has an aldehyde group, which gave us some pause as it could react with the amines of CMCHT, making them unavailable for gelation. In the event, vanillin did not harm gelation, which occurred within 1 min. The crosslinking density of the loaded hydrogel ($23.90 \pm 1.20 \times 10^{-3}$ mol/m) was comparable to that of the non-loaded hydrogel ($24.37 \pm 1.30 \times 10^{-3}$ mol/m). The lack of impact on gelation could be due to the low amount of vanillin (5 % of polymers weight). Another consideration is vanillin ionization (pKa ~ 7.4) in the PBS medium (pH 7.4) used to prepare the hydrogels (Taouri et al., 2021), increasing electron density at the vanillin aldehyde, thus reducing its reactivity with CMCHT amines. Therefore, we speculate that hydrogen bonding is responsible for the interaction between vanillin and the polymeric matrix.

In vitro release experiments were conducted in buffer solutions at pH 1.2, 5.2, and 7.4 (37 °C), selected to cover the pH range of highly to mildly acidic tumor/wound sites, and of moderately alkaline healthy tissues (Jiang et al., 2021). Cumulative vanillin release curves are shown in Fig. 10c**.** Release was rapid at all tested pH values, influenced by leaching from the hydrogel surface. Early swelling and degradation of the hydrogel matrix also contribute to the influx of release medium, and fast release of vanillin. The release rate decreased, reaching equilibrium after 12 h, revealing that the amount released was highest at pH 1.2 (82 %), followed by pH 5.2 (71 %), and pH 7.4 (63 %). Higher vanillin release at lower pH was due to the faster hydrolysis of imine crosslinks.

The mechanism of vanillin release from the hydrogel was also evaluated. Due to the fast vanillin release, the mechanism was evaluated at equilibrium (after 12 h). It was assumed that vanillin partitioned between the hydrogel and liquid phases (Reis et al., 2007). So, the release mechanism can be treated as a diffusion-partition phenomenon, which is a reasonable assumption since this kinetic analysis is done considering the equilibrium stage (Reis et al., 2007). As a result, vanillin release is governed by its partition activity (α), which is a physical-chemical parameter that represents its affinity for each phase (hydrogel, liquid medium) (de Freitas et al., 2020). To apply this model, the vanillin released fraction (F_R) and maximum released fraction (F_{max}) must be considered. Cumulative vanillin release data were fitted to first and second-order kinetic equations that take into consideration the diffusion-partition phenomenon (Fig. S30). Release data (Table 2) were better fitted by the second-order model ($R^2 \geq 0.990$), indicating that

Table 2
Kinetic parameters for release of vanillin from HEC-Ald/CMCHT hydrogel *vs.* pH (37 °C).

pH	α	First-order		Second-order	
		k_1 ($\times 10^{-4}$ h^{-1})	R^2	k_2 ($\times 10^{-4}$ h^{-1})	R^2
1.2	4.53	28.00 ± 0.29	0.973	49.40 ± 0.10	0.991
5.2	2.33	27.33 ± 0.60	0.980	41.83 ± 0.05	0.995
7.4	1.77	23.25 ± 0.01	0.984	20.68 ± 0.07	0.990

vanillin release occurred due to a combination of Fickian diffusion and controlled-relaxation mechanisms, which include swelling (*i.e.*, matrix expansion) and erosion of the hydrogel (de Freitas et al., 2020). Vanillin release was faster as release medium pH decreased. At the same time, values of α increased as the pH decreased, indicating a higher affinity of vanillin for the liquid phase. As the hydrogel expands and degrades at low pH, it cannot entrap and hold vanillin molecules, which diffuse toward the liquid phase (Reis et al., 2007). The presence of the buffer counter ions also may influence the results due to their influence on polymer conformation, but this effect is minor relative to that of pH (Zhou et al., 2023). These results confirm the pH-responsive drug release ability of HEC-Ald/CMCHT hydrogel, attractive for many biomedical applications.

3.8. Hydrogel toxicity

It is essential that potential biomaterials have minimal toxicity and do not cause undesired reactions by and in living tissues (often referred to as "biocompatibility") (Wang et al., 2020). To obtain initial insight into the suitability of the HEC-Ald/CMCHT hydrogel for biomedical applications, *in vitro* cytotoxic measurements were performed. For these experiments, normal HB4a cells (a type of breast cell line) were selected as model cells and cultured in a medium containing HEC-Ald hydrogel extract. Cell viability was evaluated by MTT assay (van de Loosdrecht et al., 1994), which measures the reduction of MTT to formazan inside cells (van de Loosdrecht et al., 1994). Formazan concentration is proportional to the number of live cells, and this molecule strongly absorbs visible light at 540 nm (van de Loosdrecht et al., 1994). Optical density (OD) measurements at 540 nm can be used to measure cell viability. Where high OD indicates high cell viability (*i.e.*, more live cells) (van de Loosdrecht et al., 1994). As assessed in Fig. 10d, the OD of cells treated with different concentrations of hydrogel is much like that of the control (without hydrogel). These results indicate that the hydrogel did not induce cell death under the experimental conditions tested, suggesting its lack of acute toxicity. Although these are promising initial results, much more evaluation in other cell lines and in *in vivo* conditions will be crucial to fully understand the "biocompatibility pathway" of this hydrogel, from first contact with the body, passing through its biological responses, and finally to clearance from the body (Williams, 2014). For example, a crucial aspect to consider is the immune response of the organism to the gelation process, *i.e.*, solidification. These factors should be considered when investigating the toxicity of *in situ* formed hydrogels, which were not evaluated in the preliminary experiments conducted. (Fig. 10d).

4. Conclusions

We have successfully demonstrated the preparation of an *in situ*-forming hydrogel by reaction of hydroxyethyl cellulose functionalized with aldehyde groups (HEC-Ald) with carboxymethyl chitosan (CMCHT), which crosslink by dynamic imine bonds.

As initially hypothesized, this strategy facilitated the efficient introduction of aldehyde groups into a non-ionic polysaccharide (in this case, HEC) without compromising the monosaccharide structure, thereby avoiding the introduction of chemical instability to the resulting derivative. However, some DP loss was still observed. The HEC-Ald derivative obtained could form a hydrogel with CMCHT in a short period (16 s). The HEC-Ald/CMCHT hydrogel also exhibited ultrafast stress relaxation, self-healing behaviors, and pH sensitivity, allowing it to control the release of encapsulated drugs. Preliminary testing revealed that the HEC-Ald/CMCHT hydrogel did not exhibit noticeable cytotoxicity against healthy cells.

All these results denote the potential applicability of this all-polysaccharide hydrogel as a potential *in situ*-forming biomaterial that may meet clinical needs by allowing localized pH-triggered release of bioactive compounds in a controlled manner. *In vivo* studies of this hydrogel also will be important to understand its behavior and performance in the clinic. Of special note, the singular ultrafast stress relaxation property observed for the prepared hydrogel is beneficial for cell growth and differentiation. Here, this property was suggested to be due to enhanced reactivity of the aldehyde groups at the termini of the oligo (hydroxyethyl) groups of the HEC derivative. An in-depth investigation into the effect of this functionalization at the termini of the oligo (hydroxyethyl) groups may offer an effective strategy to tailor the properties of the prepared hydrogel, not only stress relaxation but also gelation kinetics and mechanical properties. For instance, an interesting question is what would be the effect of the length of the oligo(hydroxyethyl) groups on the hydrogel properties? Besides that, our future studies will seek to further exploit the utility of such hydrogels in the biomedical field.

Supplementary data to this article can be found online at https://doi.org/10.1016/j.carbpol.2024.122105.

CRediT authorship contribution statement

Rafael F.N. Quadrado: Writing – original draft, Methodology, Investigation, Formal analysis, Conceptualization. **Zhenghao Zhai:** Writing – original draft, Validation, Conceptualization. **Matheus Zavadinack:** Methodology, Formal analysis. **Giseli Klassen:** Methodology, Formal analysis. **Marcello Iacomini:** Validation, Supervision. **Kevin J. Edgar:** Writing – review & editing, Writing – original draft, Validation, Supervision, Resources, Conceptualization. **André R. Fajardo:** Writing – review & editing, Supervision, Resources, Methodology.

Declaration of competing interest

The authors declare that they have no known competing financial interests or personal relationships that could have appeared to influence the work reported in this paper.

Data availability

Data will be made available on request.

Acknowledgments

The authors thank the Coordenação de Aperfeiçoamento de Pessoal de Nível Superior (CAPES/Brazil) – Finance Code 001 and PDSE fellowship (Process No. 88887.683320/2022-00). Z.Z. thanks the U.S. Department of Agriculture (NIFA), partial support through Grant 2020-67021-31379. Thanks to Brady Hall for the SEC experiments provided by GlycoMIP, a National Science Foundation Materials Innovation platform funded through Cooperative Agreement DMR-1933525. R.F.N. Q. and A.R.F. would like to express their gratitude to CAPES-Print/UFPel Program for providing the opportunity to undertake a visiting scholar period at the research group led by Prof. K.J.E.

References

Abbas, K., Amin, M., Hussain, M. A., Sher, M., Abbas Bukhari, S. N., & Edgar, K. J. (2017). Design, characterization and pharmaceutical/pharmacological applications

of ibuprofen conjugates based on hydroxyethylcellulose. *RSC Advances, 7*(80), 50672–50679. https://doi.org/10.1039/c7ra08502h
Abbas, K., Amin, M., Hussain, M. A., Sher, M., Bukhari, S. N. A., Jantan, I., & Edgar, K. J. (2017). Designing novel bioconjugates of hydroxyethyl cellulose and salicylates for potential pharmaceutical and pharmacological applications. *International Journal of Biological Macromolecules, 103*, 441–450. https://doi.org/10.1016/j.ijbiomac.2017.05.061
Arukalam, I. O., Madufor, I. C., Ogbobe, O., & Oguzie, E. E. (2014). Inhibition of mild steel corrosion in sulfuric acid medium by hydroxyethyl cellulose. *Chemical Engineering Communications, 202*(1), 112–122. https://doi.org/10.1080/00986445.2013.838158
Arya, S. S., Rookes, J. E., Cahill, D. M., & Lenka, S. K. (2021). Vanillin: A review on the therapeutic prospects of a popular flavouring molecule. *Advances in Traditional Medicine, 21*(3), 415–431. https://doi.org/10.1007/s13596-020-00531-w
Baker, A. E. G., Tam, R. Y., & Shoichet, M. S. (2017). Independently tuning the biochemical and mechanical properties of 3D Hyaluronan-based hydrogels with oxime and Diels-Alder chemistry to culture breast cancer spheroids. *Biomacromolecules, 18*(12), 4373–4384. https://doi.org/10.1021/acs.biomac.7b01422
Barham, J. P., Dalton, S. E., Allison, M., Nocera, G., Young, A., John, M. P., … Murphy, J. A. (2018). Dual roles for potassium hydride in Haloarene reduction: CSNAr and single Electron transfer reduction via organic electron donors formed in benzene. *Journal of the American Chemical Society, 140*(36), 11510–11518. https://doi.org/10.1021/jacs.8b07632
Barnes, D., & Zuman, P. (1973). Polarographic reduction of aldehydes and ketones. XV. Hydration and acid-base equilibria accompanying reduction of aliphatic aldehydes. *Journal of Electroanalytical Chemistry, 46*(2), 323–342. https://doi.org/10.1016/S0022-0728(73)80140-8
Bentley, M. D., Roberts, M. J., & Milton Harris, J. (1998). Reductive amination using polyethylene glycol acetaldehyde hydrate generated in situ: Applications to chitosan and lysozyme. *Journal of Pharmaceutical Sciences, 87*(11), 1446–1449. https://doi.org/10.1021/js980064w
Bertsch, P., Andrée, L., Besheli, N. H., & Leeuwenburgh, S. C. G. (2022). Colloidal hydrogels made of gelatin nanoparticles exhibit fast stress relaxation at strains relevant for cell activity. *Acta Biomaterialia, 138*, 124–132. https://doi.org/10.1016/j.actbio.2021.10.053
Cao, Z., Li, W., Liu, R., Li, X., Li, H., Liu, L., Chen, Y., Lv, C., & Liu, Y. (2019). pH- and enzyme-triggered drug release as an important process in the design of anti-tumor drug delivery systems. *Biomedicine and Pharmacotherapy, 118*, Article 109340. https://doi.org/10.1016/j.biopha.2019.109340
Chaudhuri, O., Gu, L., Klumpers, D., Darnell, M., Bencherif, S. A., Weaver, J. C., … Mooney, D. J. (2016). Hydrogels with tunable stress relaxation regulate stem cell fate and activity. *Nature Materials, 15*(3), 326–334. https://doi.org/10.1038/nmat4489
Chen, J., Nichols, B. L. B., Norris, A. M., Frazier, C. E., & Edgar, K. J. (2020). All-polysaccharide, self-healing injectable hydrogels based on chitosan and oxidized hydroxypropyl poly- saccharides. *Biomacromolecules, 21*(10), 4261–4272. https://doi.org/10.1021/acs.biomac.0c01046
de Freitas, C. F., Kimura, E., Rubira, A. F., & Muniz, E. C. (2020). Curcumin and silver nanoparticles carried out from polysaccharide-based hydrogels improved the photodynamic properties of curcumin through metal-enhanced singlet oxygen effect. *Materials Science and Engineering C, 112*, Article 110853. https://doi.org/10.1016/j.msec.2020.110853
Deslongchamps, P., Dory, Y. L., & Li, S. (2000). The relative rate of hydrolysis of a series of acyclic and six-membered cyclic acetals, ketals, orthoesters, and orthocarbonates. *Tetrahedron, 56*(22), 3533–3537. https://doi.org/10.1016/S0040-4020(00)00270-2
Dimatteo, R., Darling, N. J., & Segura, T. (2018). In situ forming injectable hydrogels for drug delivery and wound repair. *Advanced Drug Delivery Reviews, 127*, 167–184. https://doi.org/10.1016/j.addr.2018.03. 007
Fabbri, D., Chiavari, G., Prati, S., Vassura, I., & Vangelista, M. (2002). Gas chromatography/mass spectrometric characterisation of pyrolysis/silylation products of glucose and cellulose. *Rapid Communications in Mass Spectrometry, 16*(24), 2349–2355. https://doi.org/10.1002/rcm.856
Finkelstein, H. (1910). Darstellung organischer Jodide aus den entsprechenden Bromiden und Chloriden. *Berichte der Deutschen Chemischen Gesellschaft, 43*(2), 1528–1532. https://doi.org/10.1002/cber.19100430257
Fox, S. C., Li, B., Xu, D., & Edgar, K. J. (2011). Regioselective esterification and etherification of cellulose: A review. *Biomacromolecules, 12*(6), 1956–1972. https://doi.org/10.1021/bm200260d
Ganguly, S., Ray, D., Das, P., Maity, P. P., Mondal, S., Aswal, V. K., … Das, N. C. (2018). Mechanically robust dual responsive water dispersible-graphene based conductive elastomeric hydrogel for tunable pulsatile drug release. *Ultrasonics Sonochemistry, 42*, 212–227. https://doi.org/10.1016/j.ultsonch.2017.11.028
Gao, C., Liu, S., & Edgar, K. J. (2018). Regioselective chlorination of cellulose esters by methanesulfonyl chloride. *Carbohydrate Polymers, 193*, 108–118. https://doi.org/10.1016/j. carbpol.2018.03.093
Godoy-Alcántar, C., Yatsimirsky, A. K., & Lehn, J.-M. (2005). Structure-stability correlations for imine formation in aqueous solution. *Journal of Physical Organic Chemistry, 18*(10), 979–985. https://doi.org/10.1002/poc.941
Hozumi, T., Kageyama, T., Ohta, S., Fukuda, J., & Ito, T. (2018). Injectable hydrogel with slow degradability composed of gelatin and hyaluronic acid cross-linked by Schiff's base formation. *Biomacromolecules, 19*(2), 288–297. https://doi.org/10.1021/acs.biomac.7b01133
Jiang, X., Yang, X., Yang, B., Zhang, L., & Lu, A. (2021). Highly self-healable and injectable cellulose hydrogels via rapid hydrazone linkage for drug delivery and 3D cell culture. *Carbohydrate Polymers, 273*, Article 118547. https://doi.org/10.1016/j.carbpol.2021.118547
Lachia, M., Iriart, S., Baalouch, M., De Mesmaeker, A., & Beaudegnies, R. (2011). Ethyl-2-(2-chloroethyl)acrylate: A new very versatile α- cyclopropylester cation synthon. Efficient synthesis of cyclopropane ester derivatives by Michael addition-induced cyclization reaction. *Tetrahedron Letters, 52*(25), 3219–3222. https://doi.org/10.1016/j.tetlet.2011.04.046
Lázaro Martínez, J. M., Romasanta, P. N., Chattah, A. K., & Buldain, G. Y. (2010). NMR characteri- zation of hydrate and aldehyde forms of imidazole-2- carboxaldehyde and derivatives. *Journal of Organic Chemistry, 75*(10), 3208–3213. https://doi.org/10.1021/jo902588s
Lee, S. H., Shin, S. R., & Lee, D. S. (2019). Self-healing of cross-linked PU via dual-dynamic covalent bonds of a Schiff base from cystine and vanillin. *Materials and Design, 172*, Article 107774. https://doi.org/10.1016/j.matdes.2019.107774
Liu, A., Wu, K., Chen, S., Wu, C., Gao, D., Chen, L., … Fan, H. (2020). Tunable fast relaxation in imine-based Nanofibrillar hydrogels stimulates cell response through TRPV4 activation. *Biomacromolecules, 21*(9), 3745–3755. https://doi.org/10.1021/acs.biomac. 0c00850
Meng, Z., Zhou, X., Xu, J., Han, X., Dong, Z., Wang, H., … Liu, Z. (2019). Light-triggered in situ gelation to enable robust photodynamic-immunotherapy by repeated stimulations. *Advanced Materials, 31*(24), 1–12. https://doi.org/10.1002/adma.201900927
Nichols, B. L. B., Chen, J., Mischnick, P., & Edgar, K. J. (2020). Selective oxidation of 2-hydroxy-propyl ethers of cellulose and dextran: Simple and efficient introduction of versatile ketone groups to polysaccharides. *Biomacromolecules, 21*(12), 4835–4849. https://doi.org/10.1021/acs.biomac. 0c01045
Patenaude, M., Campbell, S., Kinio, D., & Hoare, T. (2014). Tuning gelation time and morphology of injectable hydrogels using ketone-hydrazide cross-linking. *Biomacromolecules, 15*(3), 781–790. https://doi.org/10.1021/bm401615d
Reis, A. V., Guilherme, M. R., Rubira, A. F., & Muniz, E. C. (2007). Mathematical model for the prediction of the overall profile of in vitro solute release from polymer networks. *Journal of Colloid and Interface Science, 310*(1), 128–135. https://doi.org/10.1016/j.jcis.2006.12.058
Sánchez-Morán, H., Ahmadi, A., Vogler, B., & Roh, K.-H. (2019). Oxime cross-linked alginate hydrogels with tunable stress relaxation. *Biomacromolecules, 20*(12), 4419–4429. https://doi.org/10.1021/acs.biomac.9b01100
Scheller, P. N., Lenz, M., Hammer, S. C., Hauer, B., & Nestl, B. M. (2015). Imine reductase-catalyzed intermolecular reductive amination of aldehydes and ketones. *ChemCatChem, 7*(20), 3239–3242. https://doi.org/10.1002/cctc.201500764
Silva, A. L., Babo, P. S., Rodrigues, M. T., Gonçalves, A. I., Novoa-Carballal, R., Pires, R. A., … Gomes, M. E. (2021). Hyaluronic acid oligomer immobilization as an angiogenic trigger for the neovascularization of TE constructs. *ACS Applied Bio Materials, 4*(8), 6023–6035. https://doi.org/10.1021/acsabm.1c00291
Stamps, A. C., Davies, S. C., Burman, J., & O'Hare, M. J. (1994). Analysis of proviral integration in human mammary epithelial cell lines immortalized by retroviral infection with a temperature-sensitive SV40 T-antigen construct. *International Journal of Cancer, 57*(6), 865–874. https://doi.org/10.1002/ijc.2910570616
Sun Han Chang, R., Lee, J. C. W., Pedron, S., Harley, B. A. C., & Rogers, S. A. (2019). Rheological analysis of the gelation kinetics of an enzyme cross-linked PEG hydrogel [research-article]. *Biomacromolecules, 20*(6), 2198–2206. https://doi.org/10.1021/acs.biomac.9b00116
Taouri, L., Bourouina, M., Bourouina-Bacha, S., & Hauchard, D. (2021). Fullerene-MWCNT nanostructured-based electrochemical sensor for the detection of Vanillin as food additive. *Journal of Food Composition and Analysis, 100*, Article 103811. https://doi.org/10.1016/j.jfca.2021.103811
van de Loosdrecht, A. A., Beelen, R. H. J., Ossenkoppele, G. J., Broekhoven, M. G., & Langenhuijsen, M. M. A. C. (1994). A tetrazolium-based colorimetric MTT assay to quantitate human monocyte mediated cytotoxicity against leukemic cells from cell lines and patients with acute myeloid leukemia. *Journal of Immunological Methods, 174*(1–2), 311–320. https://doi.org/10.1016/0022-1759(94)90034-5
Wang, L., Wang, C., Wu, S., Fan, Y., & Li, X. (2020). Influence of the mechanical properties of biomaterials on degradability, cell behaviors and signaling pathways: Current progress and challenges. *Biomaterials Science, 8*(10), 2714–2733. https://doi.org/10.1039/d0bm00269k
Williams, D. F. (2014). There is no such thing as a biocompatible material. *Biomaterials, 35*(38), 10009–10014. https://doi.org/10.1016/j.biomaterials.2014.08.035
Yin, H., Song, P., Chen, X., Xiao, M., Tang, L., & Huang, H. (2022). Smart pH-sensitive hydrogel based on the pineapple peel-oxidized hydroxyethyl cellulose and the Hericium erinaceus residue carboxymethyl chitosan for use in drug delivery. *Biomacromolecules, 23*(1), 253–264. https://doi.org/10.1021/acs.biomac.1c01239
Zeng, Q., Desai, M. S., Jin, H.-E., Lee, J. H., Chang, J., & Lee, S.-W. (2016). Self-healing elastin–bioglass hydrogels. *Biomacromolecules, 17*(8), 2619–2625. https://doi.org/10.1021/acs.biomac.6b00621
Zhao, Y.-J., Zhai, Y.-Q., Ma, G.-H., & Su, Z.-G. (2009). Kinetic analysis and improvement of the Williamson reaction for the synthesis of poly(ethylene glycol) propionaldehyde. *Journal of Applied Polymer Science, 111*(3), 1638–1643. https://doi.org/10.1002/app.29140
Zhou, Y., Zhai, Z., Yao, Y., Stant, J. C., Landrum, S. L., Bortner, M. J., … Edgar, K. J. (2023). Oxidized hydroxypropyl cellulose/carboxymethyl chitosan hydrogels permit pH-responsive, targeted drug release. *Carbohydrate Polymers, 300*, Article 120213. https://doi.org/10.1016/j.carbpol.2022.120213
Zott, F. L., Korotenko, V., & Zipse, H. (2022). The pH-dependence of the hydration of 5-formylcytosine: An experimental and theoretical study. *ChemBioChem, 23*(7), 1–7. https://doi.org/10.1002/cbic.202100651